Advances in Continuous and Discrete Models

RESEARCH Open Access

# Combinatorial perturbation analysis of CD4+ T cell regulatory networks based on bifurcation theory

Xiaoqi Lu[1], Qing Hu[1], Zhuozhen Xue[1] and Ruiqi Wang[1,2*]

*Correspondence:
rqwang@shu.edu.cn
[1]Department of Mathematics, Shanghai University, Shanghai, 200444, China
[2]Newtouch Center for Mathematics of Shanghai University, Shanghai, 200444, China

**Abstract**

Exploring the dynamics of the CD4+ T regulatory network holds paramount significance in scientific research, as it deepens our understanding of the immune system's intricacies and drives the development of innovative interventions for immune-related disorders. Despite the numerous studies conducted, further research is essential to elucidate the roles of exogenous cytokines in immune dynamics. This endeavor is of great importance in advancing targeted therapies and optimizing disease treatment regimens. Based on the bifurcation theory, we conduct a systematic perturbation analysis of the CD4+ T cell regulatory network. Initially, we treat exogenous cytokines as model parameters and conduct single-parameter bifurcation analysis to identify specific exogenous cytokines that can trigger various cell fate transitions. Additionally, based on relevant biological backgrounds, combinatorial perturbation analysis is performed to screen synergistic perturbation combinations. Three distinct types of synergistic combinations are successfully identified. The mechanisms by which different types of combinatorial perturbations exert their effects are also distinct. The individual and combinatorial perturbation analysis provides insights into how exogenous cytokines act synergistically and how these interactions influence the dynamics of CD4+ T cell networks.

**Keywords:** Combinatorial perturbations; Bifurcation; Synergism

## 1 Introduction

CD4+ T cells, also known as T-helper (Th) cells, play important roles in orchestrating adaptive immune responses to various infectious agents (Borst et al. [4]). They are also involved in the induction of autoimmune and allergic diseases. Naïve CD4+ T cells (Th0) differentiate into at least four subsets, Th1, Th2, Th17, and inducible regulatory T cells, each with unique functions for pathogen elimination (Fathman and Lineberry [12], Zhu and Paul [55], Christie and Zhu [10]). Th0 are activated when they recognize an antigen in a secondary lymphoid organ. Depending on the cytokine milieu and other signals in their micro-environment, CD4+ T cells attain different cell fates (Sallusto and Monticelli [43], Zhu et al. [56], Vahedi et al. [46], Yamane and Paul [49]). The seminal research by Mosmann and Coffman in the 1980s laid the groundwork by describing the Th1 and Th2

cells, two subsets of T helper cells, and elucidating the regulatory effects of their cytokine secretions on cellular and humoral immunity (Mosmann and Coffman [35]). Subsequent technological advancements allowed for further discoveries. Sakaguchi and colleagues extended the foundation by investigating regulatory T cells (Tregs), which are essential for understanding CD4+ T cell tolerance and preventing autoimmune diseases (Sakaguchi et al. [42]). Advancements in high-throughput sequencing and transcriptomics have provided us with the tools to delve deeper into CD4+ T cell gene expression patterns, clarifying the molecular underpinnings of cellular differentiation and function. Notably, the work of Zhu et al. has significantly contributed to our understanding of the transcriptional networks involved in T cell differentiation, enhancing our capability to accurately manipulate these cells for treating relevant diseases (Zhu et al. [56]). Furthermore, the research by Bettelli et al. has broadened our perspective on the diversity within CD4+ T cells through their studies on Th17 and its implication in autoimmune diseases (Bettelli et al. [3]).

When investigating the dynamics of nonlinear systems, perturbation method and bifurcation theory stand out as indispensable and crucial tools (Luongo and Paolone [31], Gorochov et al. [19], Sastry [44], Luo et al. [30], Tang et al. [45], Hu et al. [24]). They offer valuable insights into how parametric modifications can influence a system's dynamics, encompassing both quantitative and qualitative changes in its behavior. Such approaches are particularly relevant in immunological research involving CD4+ T cell networks, as they can reveal the dynamical behaviors of these cells in response to various perturbations. For instance, Yusuf et al. demonstrated the dynamical interplay between regulatory T cells (Tregs) and antigen-specific CD4+ T cells, underscoring the significance of perturbations in modulating immune responses (Yusuf et al. [51]). Additionally, Wang et al. deployed non-local reaction-diffusion models with time delays to elucidate the complex dynamics influencing CD4+ T cell population fluctuations (Wang et al. [48]). Moreover, synergistic analyses of combinatorial perturbations are acknowledged widely for their essential roles in deciphering complex systems, especially in pharmacology, where drug interactions may result in multiplicative effects. Researchers have long adopted such synergistic strategies to assess drug interactions, determining the conditions under which drug combinations yield additive, antagonistic, or synergistic effects. Their methodologies have become the cornerstone for current combination treatment strategies, directing dosage plans to maximize therapeutic efficacy while minimizing adverse effects (Chou and Talalay [9], Chou [8]). In molecular biology, synergistic perturbation analysis has been crucial for disentangling the interactions within biological pathways. Using these analyses, researchers were able to merge molecular dynamics with nuclear magnetic resonance data, illuminating the intricate interplay of proteins and ligands within cellular environments (Olivier Fisette and Morin [15]).

Furthermore, translating Boolean network models into continuous paradigms offers a more elaborate representation of biological dynamics and regulatory mechanisms (Villarreal et al. [47]). Recently, Martinez-Sanchez et al. converted Boolean networks into continuous dynamical models, enabling partial polarization and plasticity analyses within the CD4+ T cell network (Martinez-Sanchez et al. [33, 34]). A more thorough investigation is nonetheless required into how specific highly expressed molecules within continuous CD4+ T cell networks undergo alterations, as well as the synergistic impacts of exogenous cytokine combinations. Therefore, this study treats all exogenous cytokines within the CD4+ T cell regulatory network as parameters and primarily performs systematic per-

turbation and bifurcation analysis. Especially when combinatorial perturbations are applied, three distinct types of synergistic combinations are identified. The mechanisms by which different types of combinatorial perturbations exert their effects are also distinct. The analysis of both single and combinatorial perturbations offers theoretical strategies for regulating CD4+ T cell fate transitions and their control.

## 2 Material and methods

To uncover changes in highly expressed molecules that are intimately associated with various cellular states within the CD4+ T cell regulatory network, a comprehensive approach incorporating perturbation and bifurcation analysis is employed. This approach not only identifies individual cytokines but also their combinations, providing novel insights into the dynamical and intricate regulatory mechanisms that govern cell fate transitions.

### 2.1 Mathematical modeling

CD4+ T cells exhibit remarkable functional diversity and plasticity, governed by intricate regulatory networks comprising cytokines, transcription factors, and signaling molecules. These networks orchestrate the differentiation and dynamical transitions among various subsets, enabling swift adaptation to environmental cues during immune responses (Murphy and Weaver [36], Geginat et al. [17]). For instance, CD4+ T cells have the capacity to transition between Th1, Th2, Th17, or regulatory T cell (Treg) states, depending on the cytokine milieu and intracellular signaling cascades (Zhou et al. [53]). The regulatory mechanisms underlying these state transitions involve both deterministic and stochastic processes, making mathematical modeling an essential tool for understanding their dynamics. Specifically, ordinary differential equations (ODEs) offer a suitable framework for modeling the complex nonlinear regulations between cytokines and transcription factors within these networks (Hirsch [23], Fischer [14], Perko [41]). Without loss of generality, we consider an $n$-node network whose dynamics can be described by

$$\frac{dx}{dt} = f(x;p), \tag{1}$$

where $x = (x_1, x_2, \ldots, x_n)^T \in R^n$ is a vector of nodes, which represents concentrations of all molecules, $f = (f_1, f_2, \ldots, f_n)^T$ is a vector of functions representing the regulations between individual molecules, and the parameter vector $p = (p_1, \ldots, p_m)^T \in R^m$ represents environmental conditions which can be perturbed individually or combinatorially so as to change or control the system dynamics.

The CD4+ T cell regulatory network consists of 21 nodes (Martinez-Sanchez et al. [33]), as shown in Fig. 1. The five nodes at the bottom (blue rectangles) represent transcription factors: TBET, GATA3, FOXP3, RORGT, and BCL6. The seven central nodes (blue ovals) represent signaling pathways that integrate signal transducers, including STAT proteins, interleukin receptors, and autocrine cytokines, specifically IFNG, IL2, IL4, IL10, TGFB, IL9, and IL21. The nine topmost nodes (pink diamonds) signify exogenous cytokines generated by distinct cells within the immune system. Consequently, as input signals to the network, these functions comprise IFNGe, IL12e, IL2e, IL4e, IL10e, IL27e, TGFBe, IL6e, and IL21e. These cytokines are distinctively identified by an "e" suffix (denoting exogenous) to clearly distinguish them as externally produced cytokines serving as inputs to the network.

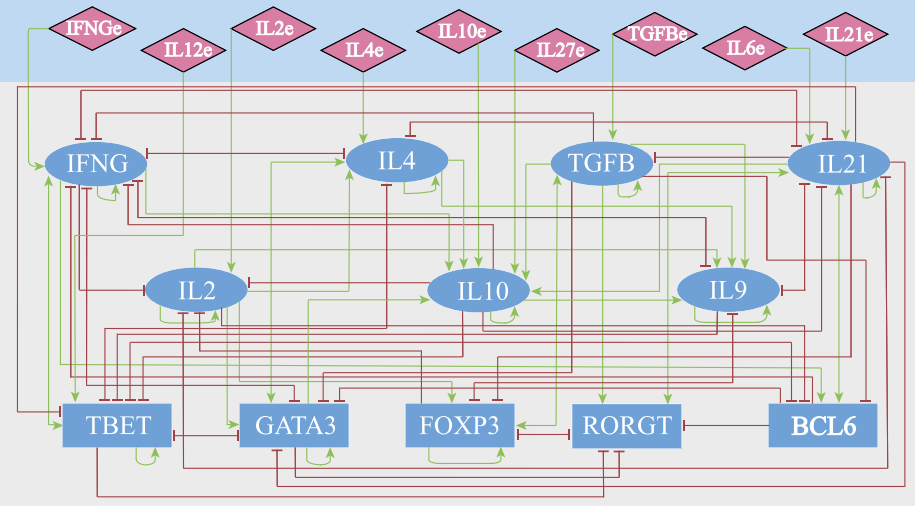


**Figure 1** CD4+ T cell regulatory network. The network includes transcription factors (rectangles), signaling pathways and autocrine cytokines, autocrine cytokines (ovals), and exogenous cytokines (diamonds). Activation is represented by green arrows, while inhibition is represented by red flat arrows. In the dynamic model, the transcription factors and autocrine cytokines serve as state variables, whereas exogenous cytokines are represented as parameters

We select nine exogenous factors as the parameter vector $p$ and other molecules as the system variables $x$. For the construction of the CD4+ T cell regulatory network, as well as the identification of key highly expressed cytokines, please refer to (Martinez-Sanchez et al. [33, 34]) for more details. It is worth noting that the Th0 cell state encompasses two distinct yet stable precursor states (Th1/Th2 precursors), characterized by the absence of cytokine expression, with the exception of IL2. However, upon reaching an optimal level of IL2e, i.e., mathematically, under the perturbation to IL2e, a bifurcation occurs, leading to a significant up-regulation of IL2 expression. Therefore, we deliberately divide the Th0 state into Th0 and Th0_2, as shown in Table 1. Similarly, in order to more clearly reflect the state transition under relevant perturbations, we also divide the Th2 state into two states: Th2 and Th2_2, as shown in Table 1 and Table 2.

The regulatory function $f$ between individual molecules and the specific ODEs of the CD4+ T network are given in the Appendix.

## 2.2 Perturbation analysis based on bifurcation

Cell fate transition stands as a pivotal milestone in organismal development, intricately shaping the diversity and functionality of cells. In unraveling the intricate regulatory process, the bifurcation and perturbation analysis of nonlinear dynamical systems are crucial analytical methods. They can offer profound insights into the intricate dynamics of gene expression, thereby facilitating a deeper understanding of how cells adopt their distinct identities and roles within the organism (Bargaje et al. [1], Bose and Pal [5]).

From the perspective of nonlinear dynamics, cell fate transition can be regarded as a bistable or ultrasensitive switch, intricately guiding the complex transitions among diverse cellular identities (Nakajima and Kaneko [38], Marco et al. [32]). When a certain parameter, such as the concentration of a signaling molecule, reaches a critical value, a bifurcation occurs, inducing the transition from one cell state to another. This state transition process

may involve complex dynamics, such as periodic oscillations and chaos, which can all be systematically studied using bifurcation analysis.

In this study, our model consists of a set of nonlinear ODEs that describe the regulations among transcription factors, signaling pathways, and autocrine cytokines within the CD4+ T cell network. To determine the steady states of different T cell subtypes (e.g., Th0, Th1, Th2, Th3, Tfh, and Tr1) under specific environmental conditions, we employ numerical simulation methods. The stable, steady state is identified as the state where the changes in system variables tend towards zero over a sufficient period of time.

In the combinatorial perturbation analysis, we examine the effects of simultaneous perturbation on two parameters. The primary concern is to evaluate how the fate of CD4+ T cells is altered in response to simultaneous changes in multiple exogenous cytokines. Specifically, we utilize the mathematical tool MATCONT, which is widely applied in the analysis of bifurcations within dynamical systems. By defining the parameter ranges and step sizes, we can accurately capture vital information during the bifurcation analysis. This methodology allows us to detect bifurcation points or loci within the parameter spaces, indispensable for understanding the qualitative changes in system dynamics.

In the subsequent sections, we will analyze the intricate dynamics of the CD4+ T cell regulatory network, utilizing bifurcation and perturbation analysis. The detailed methodologies employed are outlined as follows.

### *2.2.1 Acquisition of initial steady state*

Table 1 presents various CD4+ T cell types, Th0_2, Th1, Th2 (Perez et al. [40], Kanhere et al. [27]), Th3 (Gol-Ara et al. [18]), Tfh (Johnston et al. [25]), Tr1 (Grazia Roncarolo et al. [20]), along with their corresponding highly expressed cytokines and active input nodes. In this context, the high expression level $x_{\text{high}}$ is defined as $x \in [0.5, 1]$, whereas the low expression level $x_{\text{low}}$ is defined as $x \in [0, 0.5)$. According to Table 1, for each cellular phenotype, we set $x_{\text{high}} = 0.7$, $(i = 1, \ldots, n_{\text{high}})$ and $x_{\text{low}} = 0.1$, $(i = 1, \ldots, n_{\text{low}})$, where $n_{\text{high}}$ and $n_{\text{low}}$ denote the number of cytokines corresponding to high and low expression levels in each state, respectively. By setting the parameter vector $\mathbf{p} = 0$, we can calculate the steady-state data corresponding to each phenotype. It is important to note that the Tr1 phenotype requires the involvement of exogenous cytokines, i.e., IL27e and IL10e. Specifically, their values can be set to 0.6 and 0.4, respectively, to obtain the steady-state solutions for the Tr1 phenotype.

### *2.2.2 Single-parameter perturbation*

We consider all exogenous cytokines as a parameter set: $P = \{p_1, p_2, \ldots, p_9\}$. In each single-parameter perturbation, the parameters are divided into two subsets: the perturbed parameter set: $S_1 = \{p_i\}$, $p_i \in P$, and the non-perturbed parameter set (kept constant):

**Table 1** Distinct cell states, key highly expressed cytokines, and corresponding exogenous cytokines

| Cell states | Highly expressed cytokines | Active input nodes |
|---|---|---|
| Th0 | - | - |
| Th0_2 | IL2 | IL2e |
| Th1 | TBET, IFNG | IL12e, IFNGe |
| Th2 | GATA3, IL4 | IL4e |
| Th3 | TGFB | TGFBe |
| Tfh | IL21, BCL6 | IL6e, IL21e |
| Tr1 | IL10 | IL10e, IL27e |

$S_2 = P \setminus S_1$. Under this setup, the dynamical system Eq. (1) can be expressed as:

$$\frac{dx}{dt} = f(x, p_i, p_{\text{fixed}}), \tag{2}$$

where:

- $p_i$: the perturbed parameter, which typically varies within a specific range, i.e., $p_i \in [p_{i,\min}, p_{i,\max}]$. In this study, $p_{i,\min} = 0$, $p_{i,\max} = 1$;
- $p_{\text{fixed}} = [p_j \mid p_j \in S_2]$: the nonperturbed parameters. The unperturbed parameters are set to zero, unless stated otherwise.

By adjusting the value of $p_i$, we study the system's dynamics, such as steady-state solutions $x^*$ or bifurcation. The steady-state solution satisfies the following condition: $f(x^*, p_i, p_{\text{fixed}}) = 0$, where $x^*$ is the steady-state solution corresponding to the parameter $p_i$.

#### *2.2.3 Combinatorial perturbations*

In the case of two-parameter perturbations, the parameter set $P$ is divided into two subsets:

- The perturbed parameter set: $S_1 = \{p_a, p_b\}$, $p_a, p_b \in P$, where $p_a$ and $p_b$ are the two parameters subjected to simultaneous perturbation.
- The nonperturbed parameter set (kept constant): $S_2 = P \setminus S_1 = \{p_k \mid p_k \in P, p_k \notin S_1\}$. These parameters remain fixed during the analysis.

Under two-parameter perturbations, the dynamical system can be written as:

$$\frac{dx}{dt} = f(x, p_a, p_b, p_{\text{fixed}}), \tag{3}$$

where:

- $p_a$ and $p_b$: the two perturbed parameters, which vary within specified ranges: $p_a \in [p_{a,\min}, p_{a,\max}]$ and $p_b \in [p_{b,\min}, p_{b,\max}]$;
- $p_{\text{fixed}} = [p_k \mid p_k \in S_2]$: the set of nonperturbed parameters, which remains constant.

The steady-state solution satisfies the following condition: $f(x^*, p_a, p_b, p_{\text{fixed}}) = 0$, where $x^*$ is the steady state, which depends on the parameter values of $p_a$ and $p_b$.

## 3 Results

Our primary objective in this section is to identify distinct cell states within the CD4+ T cell network, utilizing key, highly expressed cytokines as indicators of cellular states. To explore the dynamics of cell transitions between these diverse fates, we employ perturbation and bifurcation analysis as our analytical approaches.

### 3.1 Single-parameter perturbation analysis

Exogenous cytokines, i.e., active input (rightmost column), can induce different cell state transformations (leftmost column), as shown in Table 1. The middle column corresponds to the highly expressed cytokines under the specific perturbations. In this subsection, we explore how these highly expressed cytokines change under individual perturbations. We first perturb the parameters IL12e, IFNGe, IL2e, IL4e, IL6e, IL21e, TGFBe, IL10e, and IL27e, respectively. These specific individual perturbations induce different system dynamics, e.g., bistable and ultrasensitive switches, as shown in Fig. 2.

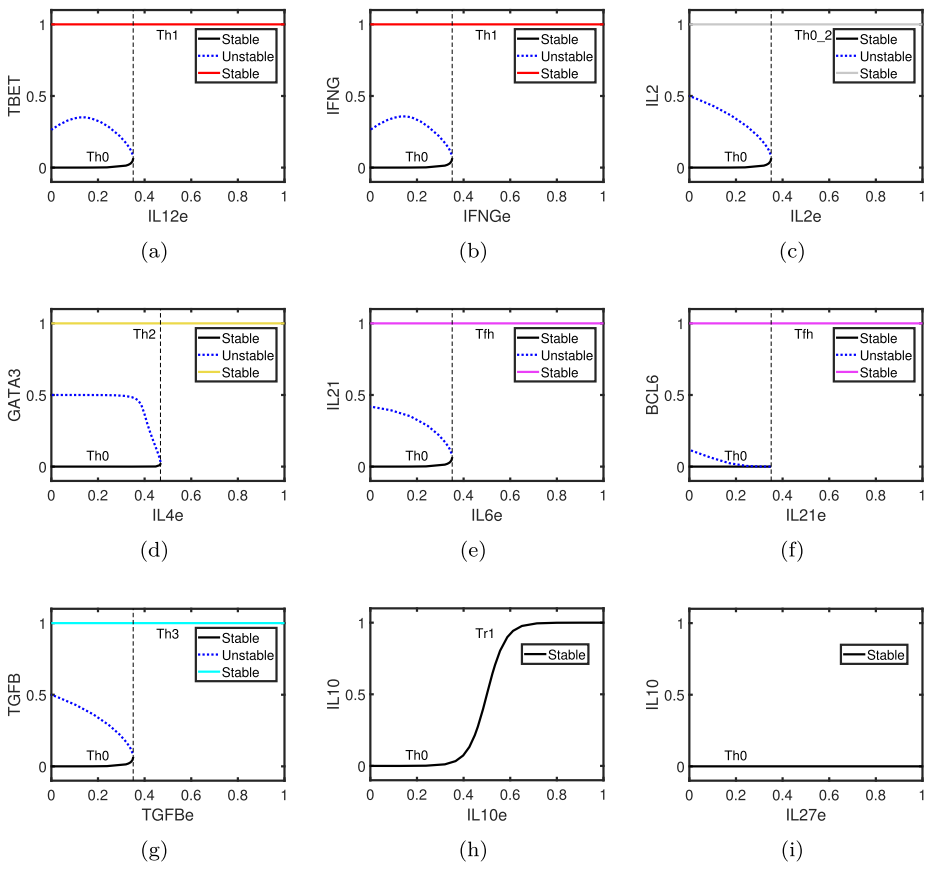


**Figure 2** The dynamics under individual perturbations. (a)–(d) Bistable switches under the perturbations to IL12e, IFNGe, IL2e, IL4e, IL6e, IL21e, and TGFBe. (h) Ultrasensitive switch under the perturbation to IL10e. (i) The perturbation to IL27e does not induce any state transition

When the system resides in the Th0 state, the gradual increase in IL12e level triggers a modest increase in the TBET expression, maintaining the system's stability within the Th0 state. However, upon reaching a threshold of approximately 0.35, the system undergoes a bifurcation characterized by an abrupt jump in the TBET expression. This critical occurrence marks a transition from the Th0 to the Th1 state, as illustrated in Fig. 2(a). As IL12e continues to increase, the expression level of TBET remains unchanged, and the system remains in the Th1 state.

The system demonstrates the phenomenon of bistability within the interval of $[0, 0.35]$, indicating its ability to maintain two stable states concurrently. From a biological perspective, when a cell remains in the Th0 state and is continuously exposed to the exogenous cytokine IL12e, it does not initially undergo any immediate apparent change in its state. However, upon reaching a critical threshold concentration of IL12e, the cell undergoes a definitive transition in its fate, shifting from the Th0 state to the Th1 state. Conversely, when the cell remains in the Th1 state, the decrease or absence of the external cytokine IL12e does not trigger a return to the Th0 state, highlighting the one-way or irreversible nature of the cell fate transition.

Similarly, various exogenous cytokines such as IFNGe, IL2e, IL4e, IL6e, IL21e, or TGFBe can induce distinct cell fate transitions through saddle-node bifurcations. For instance,

exogenous cytokine IFNGe can also trigger the transitions from Th0 to the Th1 state, whereas exogenous cytokine IL4e, IL6e, or TGFBe can respectively induce the cell fate transition from Th0 to Th2, Tfh, or Th3 state, as shown in Figs. 2(b)–2(g). However, exogenous cytokine IL10e induces an ultrasensitive switch, as shown in Fig. 2(h). As the concentration of IL10e increases, the expression of IL10 follows an S-shaped pattern, indicating a substantial change in IL10 level. This response is indicative of an ultrasensitive response mechanism (Haney et al. [22], Ferrell and Ha [13], Zhang et al. [52]). In contrast, exogenous cytokine IL27e does not lead to any bifurcation, thereby precluding any cell fate transition. Despite IL10 being a target of IL27e, the expression of IL10 remains largely insensitive to variations in IL27e concentration, as shown in Fig. 2(i).

### 3.2 Combinatory perturbation analysis

During cell fate transitions, synergistic effects of combinatorial perturbations are crucial. Multiple exogenous cytokines can interact to synergistically regulate gene expression and determine cell fate transitions (Yan et al. [50], Choi et al. [7]). In this part, we identify three different types of synergistic effects of exogenous cytokines on cell fate transitions by combinatorial perturbation analysis. Type I: those parameters which, when individually perturbed, do not cause any bifurcation i.e., (IL10e, IL27e) (Murugaiyan et al. [37]); Type II: those parameters which, when individually perturbed, induce the same types of cell fate transitions, i.e., (IL12e, IFNGe) (Lexberg et al. [29]) and (IL6e, IL21e) (Eto et al. [11]); and Type III: those parameters which, when individually perturbed, induce the different types of cell fate transitions, i.e., (IL2e, TGFBe) (Freudenberg et al. [16]), (IL2e, IL4e) (Burke et al. [6]), (IL4e, TGFBe) (Beriou et al. [2]) and (IL21e, TGFBe) (Zhou et al. [54]), as outlined in Table 2.

#### *3.2.1 Type I*

The single perturbation to IL10e induces the fate transition from Th0 to Tr1 by an ultrasensitive switch, as shown in Fig. 2(h). The single perturbation to IL27e does not induce any bifurcation and therefore no cell fate transitions occur, as shown in Fig. 2(i). However, when they are simultaneously perturbed, saddle-node bifurcations occur, meaning the occurrence of cell fate transitions, as shown in Fig. 3(a).

In order to explore the intricate relationship between simultaneous perturbations to IL10e and IL27e, when perturbing IL10e, we systematically vary the levels of IL27e, setting its values to 0, 0.28, 0.5, and 0.8, respectively. When IL27e = 0.28, two saddle-node

**Table 2** Three combination types, cell states, and highly expressed cytokines under combinatorial perturbations

| Types | Combinatorial perturbations | Cell states | Highly expressed cytokines |
|---|---|---|---|
| Type I | (IL10e, IL27e) | Tr1 | IL10 |
| Type II | (IL12e, IFNGe) | Th1 | TBET, IFNG |
| | (IL6e, IL21e) | Tfh | IL21, BCL6 |
| Type III | (IL2e, IL4e) | Th2_2 | GATA3, IL2, IL4 |
| | (IL21e, TGFBe) | Th17 | RORGT, IL21, TGFB |
| | (IL2e, TGFBe) | iTreg | IL2, IL4, FOXP3, TGFB |
| | (IL4e, TGFBe) | Th9 | IL4, TGFB, IL9, IL10 |

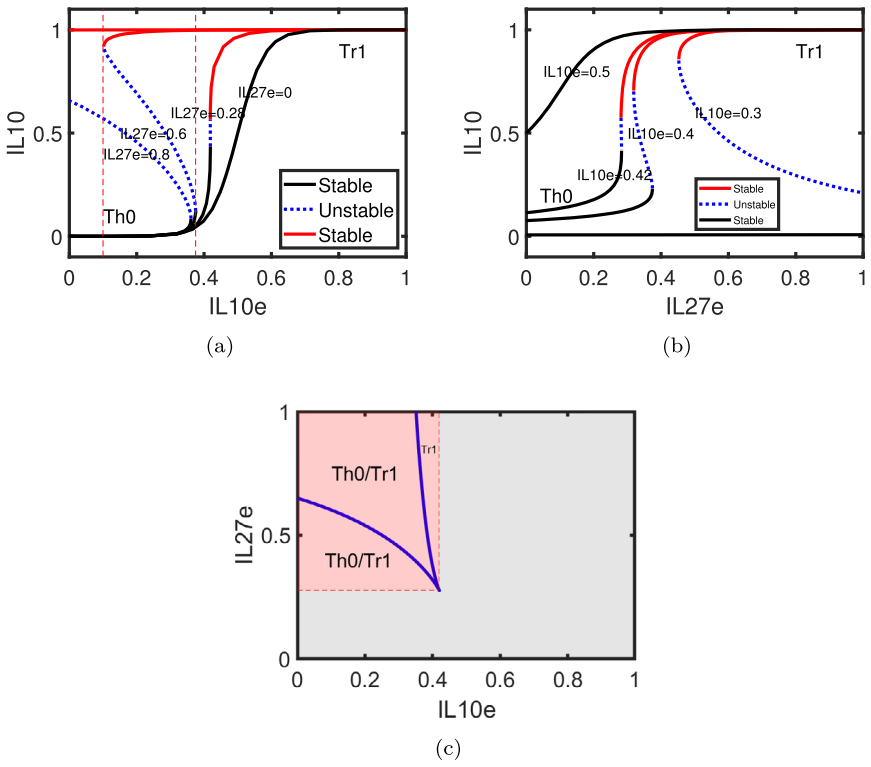


**Figure 3** Combinatorial perturbation analysis. (a) The perturbation to IL10e when IL27e is 0, 0.28, 0.6, and 0.8, respectively. (b) The perturbation to IL27e when IL10e is 0.3, 0.4, 0.42, and 0.5 respectively. (c) The bifurcation diagram of combinatorial perturbations to IL10e and IL27e

bifurcation points nearly coincide. This approach allows us to obtain a comprehensive understanding of how these two exogenous cytokines influence each other under different conditions. As the perturbation to IL27e is strong enough, saddle-node bifurcations may occur. In addition, as the concentration of IL27e rises, the bifurcation occurs earlier, suggesting an enhanced sensitivity to the perturbation to IL10e, as shown in Fig. 3(a). Especially when IL27e reaches a sufficiently high level, the cell fate transition becomes irreversible. In other words, only the transition from Th0 to Tr1 is possible.

Similarly, we perturb IL27e by adjusting IL10e at different levels (specifically, 0.3, 0.4, 0.42 and 0.5). As IL10e increases, the initial response in IL27e exhibits bifurcation. However, the bifurcation subsequently diminishes, and the system undergoes a gradual, continuous change, as shown in Fig. 3(b). The two-parameter bifurcation diagram is shown in Fig. 3(c). The pink background region signifies the occurrence of bifurcation during the perturbation process, whereas the gray region denotes the absence of bifurcation, indicating that the system undergoes continuous changes.

In summary, when both perturbations are imposed, the transition occurs via saddle-node bifurcations, indicating the synergistic effects of the combinatorial perturbations in the CD4+ T cell regulatory network. Two perturbations cooperate to compensate for respective inefficiency in inducing the bistable switch and thus the transition from Th0 to Tr1. During the transition, the perturbation to IL10e plays a decisive role, while the perturbation to IL27e functions as an auxiliary factor.

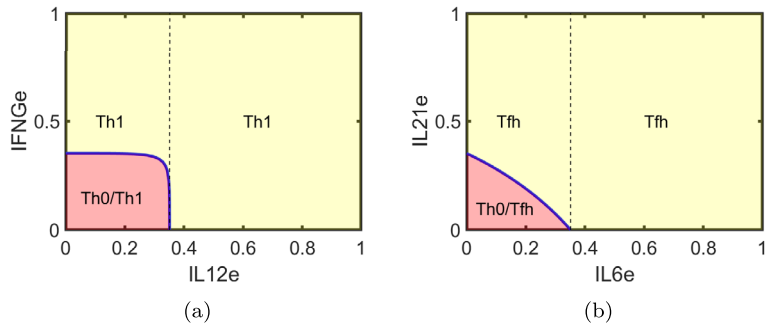


**Figure 4** Combinatorial perturbation analysis. (a) The two-parameter bifurcation diagram when IL2e and IFNGe are simultaneously perturbed. (b) The two-parameter bifurcation diagram when IL6e and IL21e are simultaneously perturbed

### *3.2.2 Type II*

A single perturbation to IL27e fails to induce any discernable cell fate transition, whereas an isolated perturbation to IL10e triggers an ultrasensitive switching mechanism. However, when both IL27e and IL10e are simultaneously perturbed, they collaborate to facilitate cell fate transitions through bistable switches. Additionally, some individual perturbations can independently induce specific cell fate transitions, as shown in Figs. 2(a)–(h). For instance, a single perturbation to IL12e or IFNGe can drive the transition from Th0 to Th1, while a single perturbation to IL21e or IL6e can realize the transition from Th0 to Tfh.

For combinatorial perturbations, the interplay between IL12e and IFNGe in inducing the transition from Th0 to Th1 is depicted in the two-parameter bifurcation diagram (Fig. 4(a)). Similarly, the combinatorial effects of IL21e and IL6e on the transition from Th0 to Tfh are shown in Fig. 4(b). In both cases, the perturbations exhibit a negative correlation, where an increase in one reduces the requirement for the other to achieve the transitions. These findings highlight how the perturbations compensate for each other's inefficiencies in inducing cell fate transitions.

Specifically, for the Th0-to-Th1 transition, an additional perturbation to IL12e reduces the requirement for IFNGe and vice versa. Similarly, for the Th0-to-Tfh transition, IL21e and IL6e cooperate, with each perturbation mitigating the need for the other. In Type II combinatorial perturbations, both components play similar roles in facilitating cell fate transitions by lowering the bifurcation thresholds when introduced simultaneously.

### *3.2.3 Type III*

Combinatorial perturbations not only orchestrate the system's state in a synergistic manner but also produce potentially novel cell states. Here, we focus on four combinatorial perturbations: (IL2e, TGFBe), (IL2e, IL4e), (IL4e, TGFBe), and (IL21e, TGFBe), which are comprehensively outlined in Table 2. These cytokine combinations offer insights into intricate mechanisms of combinatorial regulations, which can drive the system towards other functional states.

A. Combinatorial perturbations to IL2e and TGFBe

When IL2e is imposed, the cell fate transition from Th0 to Th0_2 can be realized, as shown in Fig. 2(c). At an appropriate concentration of TGFBe, the cell fate transition from

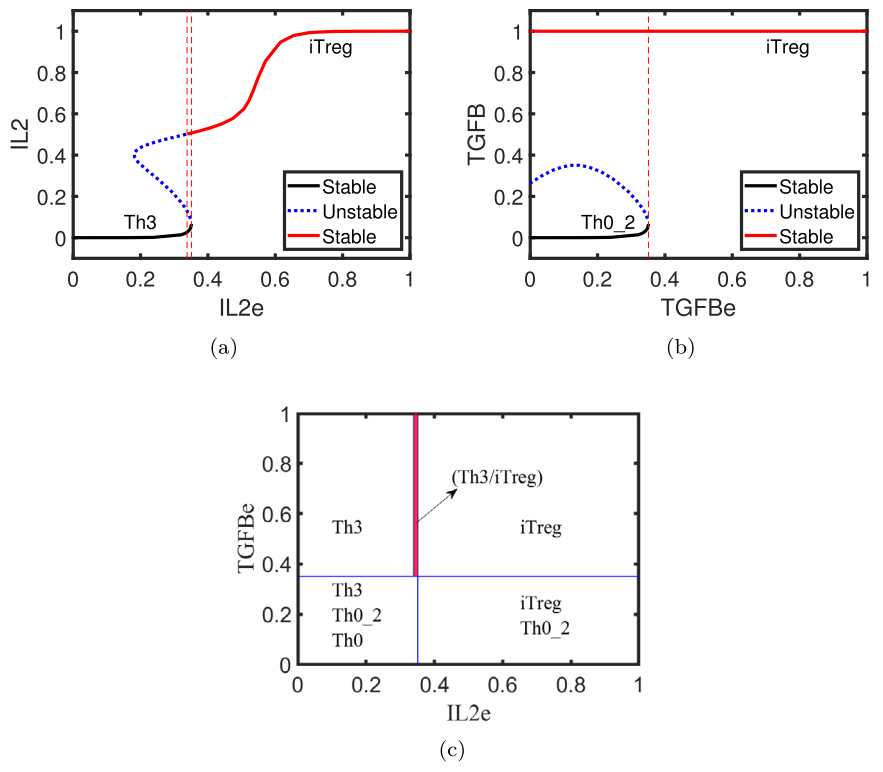


**Figure 5** Combinatorial perturbation analysis. (a) The bifurcation diagram with IL2e as the control parameter at TGFBe = 0.6. (b) The bifurcation diagram with TGFBe as the control parameter at IL2e = 0.6. (c) The bifurcation diagram of combinatorial perturbations to IL2e and TGFBe

Th0 to Th3 can be achieved, as shown in Fig. 2(g). Following this, we perform combinatorial perturbation analysis. For instance, at TGFBe = 0.6, the system stabilizes in the Th3 state (Fig. 2(g)). However, when an additional perturbation to IL2e is applied under this condition, the system transitions from the Th3 state to the iTreg state (Fig. 5(a)).

Similarly, at IL2e = 0.6, the system stabilizes in the Th0_2 state (Fig. 2(c)). Upon the introduction of a further perturbation to TGFBe, the system transitions from the Th0_2 state to the iTreg state (Fig. 5(b)). These results indicate that the transition from Th0 to iTreg can only be realized through combinatorial perturbations.

The transition from the Th0 state to the iTreg state is facilitated through either the Th0_2 or Th3 intermediate state, depending on the specific combination and manner of the perturbations employed (Fig. 5(c)). These findings emphasize the critical roles of combinatorial perturbations in uncovering synergistic effects and inducing novel cell states.

B. Combinatorial perturbations to IL2e and IL4e

When IL4e is applied at an optimal concentration, the cell fate transition from Th0 to Th2 can be successfully achieved, as demonstrated in Fig. 2(d). The single perturbation to IL2e induces a transition within the Th0 lineage, particularly to a state resembling Th0 but with high levels of IL2, as shown in Fig. 2(c). Different individual perturbations lead to distinct cell fate transitions. Through combinatorial perturbations, the transition from Th0 to Th2_2 can be effectively achieved. For instance, at IL4e = 0.6, the system stabilizes in the Th2 state (Fig. 2(d)). Upon the application of additional perturbations, the system transitions from Th2 to Th2_2 (Fig. 6(a)).

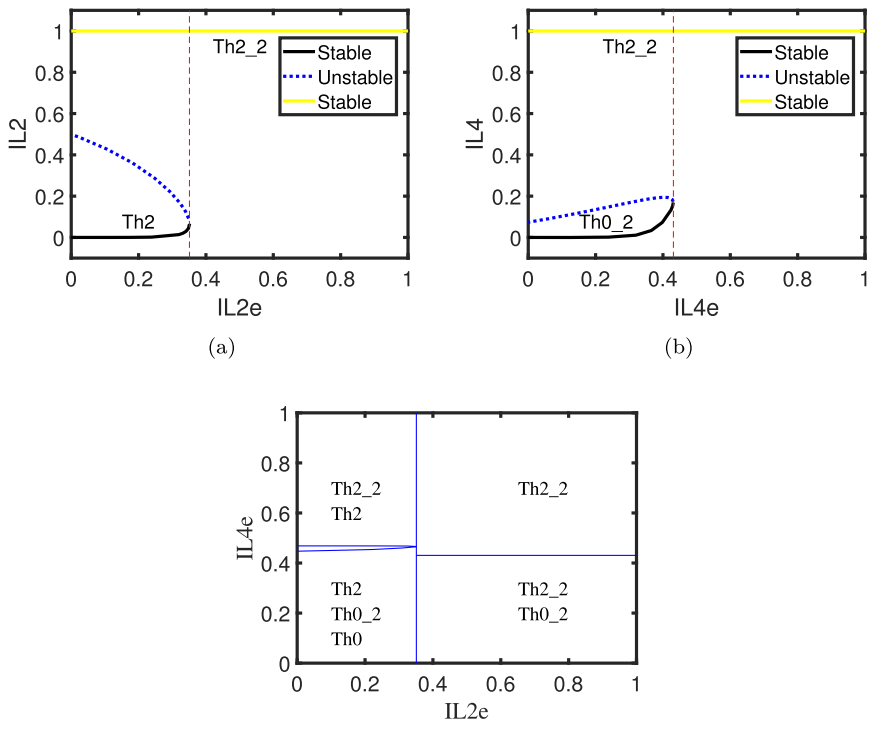


**Figure 6** Combinatorial perturbation analysis. (a) The bifurcation diagram with IL2e as the control parameter at IL4e = 0.6. (b) The bifurcation diagram with IL4e as the control parameter at IL2e = 0.6. (c) The bifurcation diagram of combinatorial perturbations to IL2e and IL4e

Similarly, at IL2e = 0.6, the system remains in the Th0_2 state (Fig. 2(c)). When the perturbation to IL4e is further introduced, the system undergoes a transition from the Th0_2 state to the Th2_2 state, as shown in Fig. 6(b).

These findings demonstrate that the transition from Th0 to Th2_2, which cannot be achieved by individual perturbation to IL2e or IL4e alone, requires the synergistic action of both cytokines in combinatorial perturbations and can proceed via either Th2 or Th0_2 intermediate states, depending on how the perturbations are applied (Fig. 6(c)).

C. Combinatorial perturbations to IL4e and TGFBe, and to IL21e and TGFBe

The exogenous cytokine IL4e can induce the cell fate transition from Th0 to Th2, as shown in Fig. 2(d). While exogenous cytokine TGFBe can realize the cell fate transition from Th0 to Th3, as shown in Fig. 2(g). Different individual perturbations induce different cell fate transitions. When combinatorial perturbations are performed, the cell fate transition from Th0 to Th9 can be realized. For instance, at a strong enough TGFBe level, e.g., TGFBe = 0.6, the further transition from Th3 to Th9 is realized through an ultrasensitive switch which enables sharp transitions between two different cell states and is essential for cells to respond to environmental cues with high fidelity, as shown in Fig. 7(a). Similarly, at the concentration of IL4e = 0.6, the system remains in the Th2 state, as shown in Fig. 2(d). When the perturbation to TGFBe is further introduced, the system undergoes a transition from the Th2 state to the Th9 state, as shown in Fig. 7(b). These findings demonstrate that the transition from Th0 to Th9 can be effectively achieved through combinatory perturbations. The transition from Th0 to Th9 can be accomplished via either

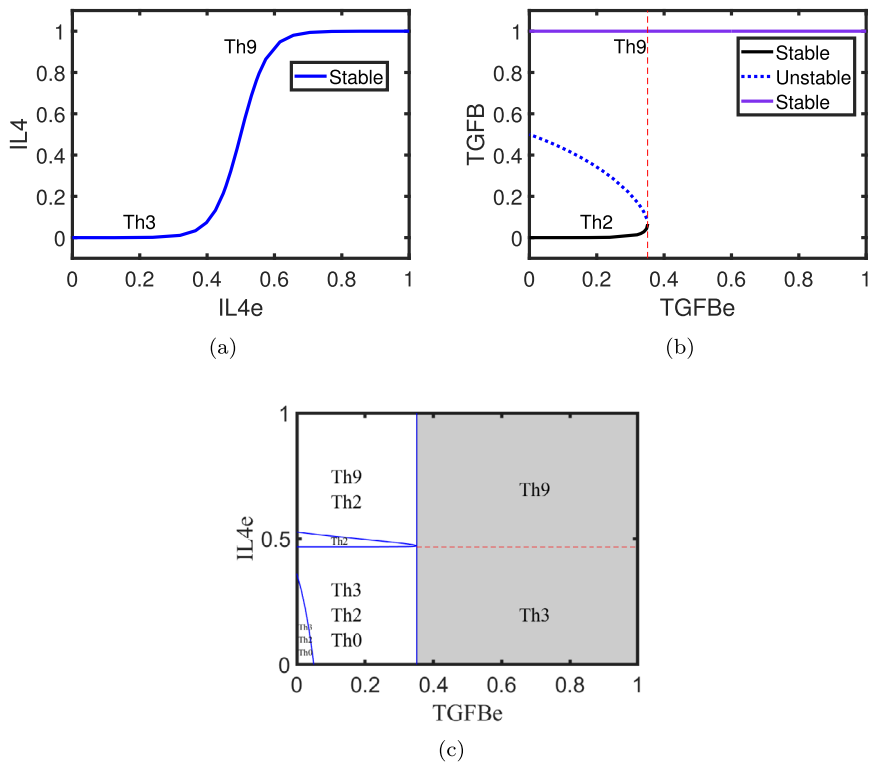


**Figure 7** Combinatorial perturbation analysis. (a) The ultrasensitive switch induced by the perturbation to IL4e at TGFBe = 0.6. (b) The bifurcation diagram with TGFBe as the control parameter at IL4e = 0.6. (c) The dynamics under the combinatorial perturbations to IL4e and TGFBe

Th2 or Th3 intermediate, depending on the specific manners in which the combinatorial perturbations are applied, as shown in the two-parameter bifurcation diagram Fig. 7(c).

The exogenous cytokine IL21e can induce the cell fate transition from Th0 to Tfh, as shown in Fig. 2(f). While exogenous cytokine TGFBe can realize the cell fate transition from Th0 to Th3, as shown in Fig. 2(g). When combinatorial perturbations are performed, the cell fate transition from Th0 to Th17 can be realized. For instance, at a strong enough IL21e level, e.g., IL21e = 0.6, the further transition from Tfh to Th17 is realized through an ultrasensitive switch, as shown in Fig. 8(a). Similarly, at the concentration of TGFBe = 0.6, the system remains in the Th3 state, as shown in Fig. 2(g). When the perturbation to IL21 is further introduced, the system undergoes a transition from the Th3 state to the Th17 state, as shown in Fig. 8(b). These findings demonstrate that the transition from Th0 to Th9 can be effectively achieved through combinatory perturbations. The transition from Th0 to Th17 can be accomplished via either Th3 or Tfh intermediate, depending on the specific manners in which the combinatorial perturbations are applied, as shown in the two-parameter bifurcation diagram Fig. 8(c).

In summary, during the induction of cell fate transitions, three distinct combinatorial perturbations exhibit synergistic yet different mechanisms. Specifically, for the first type, only the single perturbation to IL10e is sufficient to elicit the transition from Th0 to Tr1 cell fate. The addition of exogenous cytokine IL21e functions as an adjuvant, facilitating the transition process from Th0 to Tr1 and making the transition easier. For the second type, each individual perturbation is capable of independently achieving the transition. In

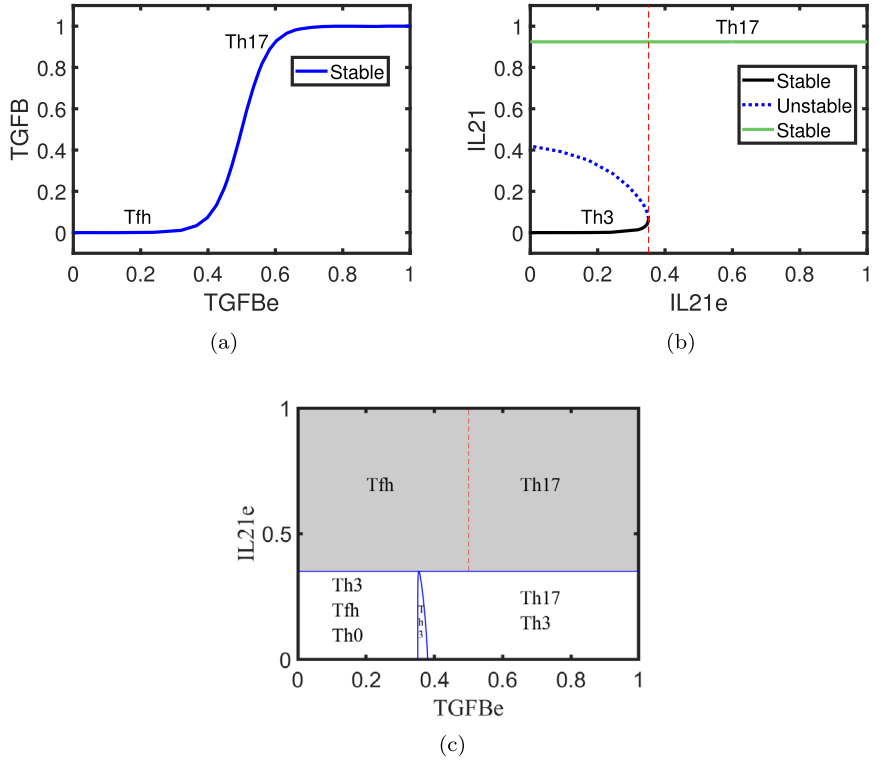


**Figure 8** Combinatorial perturbation analysis. (a) The ultrasensitive switch induced by the perturbation to TGFBe at IL21e = 0.6. (b) The bifurcation diagram with IL21e as the control parameter at TGFBe = 0.6. (c) The dynamics under the combinatorial perturbations to IL21e and TGFBe

addition, when combined, these perturbations exhibit a synergistic effect, with both cytokines collaborating to facilitate the same type of cell fate transition even more efficiently. Regarding the third type, within each perturbation pair, each distinct perturbation triggers a different cell fate transition. Furthermore, combinatorial perturbations work synergistically and give rise to novel cell fate transitions.

## 4 Conclusion and discussion

This study conducts a dynamic analysis of the CD4+ T cell regulatory network, employing nonlinear dynamics and bifurcation theory. Initially, we carried out single-parameter perturbations on nine exogenous cytokines. The system undergoes bifurcation when individually perturbing IL12e, IFNGe, IL2e, IL4e, IL6e, IL21e, and TGFBe. Specifically, an ultrasensitive switch occurs under the perturbation to IL10e. These single-parameter perturbation analyses provide valuable insights for further combinatorial perturbation analysis.

When combinatorial perturbations are applied, three distinct types of synergistic combinations are identified. Specifically, in the first type of combination, only one perturbation is sufficient to induce a cell fate transition, while the addition of another exogenous cytokine acts as an adjuvant, enhancing and facilitating the process. In the second type, each individual perturbation can independently induce cell fate transitions. When combined, they collaborate to facilitate the same type of transition even more efficiently. As for the third type, within each pair of perturbations, each distinct perturbation triggers a

different cell fate transition. Also, when combined synergistically, these perturbations give rise to novel cell fate transitions.

The analysis of both single and combinatorial perturbations offers theoretical strategies for regulating CD4+ T cell fate transitions (O'Shea and Paul [39], Geginat et al. [17]). The methodology presented herein can be extended to other biological networks to uncover crucial mechanisms or molecules pertinent to cell fate decisions and transitions. Furthermore, it may aid in the design of novel combinatorial perturbations, thereby presenting fresh perspectives for targeted therapeutic strategies (Haghverdi et al. [21], Kakaradov et al. [26], Lähnemann et al. [28]). Nevertheless, there remains room for improvement. Specifically, the network nodes are restricted, and the ODE model grounded in Boolean networks has the potential for further enhancement.

## Appendix: The model

The dynamics of CD4+ T cell network is described by ODEs as follows (Martinez-Sanchez et al. [33]):

$$\begin{aligned}
\frac{d[TBET]}{dt} &= \frac{1}{1+exp(-b*(w_{TBET}-0.5))} - k_{TBET}*[TBET],\\
\frac{d[IFNG]}{dt} &= \frac{1}{1+exp(-b*(w_{IFNG}-0.5))} - k_{IFNG}*[IFNG],\\
\frac{d[GATA3]}{dt} &= \frac{1}{1+exp(-b*(w_{GATA3}-0.5))} - k_{GATA3}*[GATA3],\\
\frac{d[IL2]}{dt} &= \frac{1}{1+exp(-b*(w_{IL2}-0.5))} - k_{IL2}*[IL2],\\
\frac{d[IL4]}{dt} &= \frac{1}{1+exp(-b*(w_{IL4}-0.5))} - k_{IL4}*[IL4],\\
\frac{d[RORGT]}{dt} &= \frac{1}{1+exp(-b*(w_{RORGT}-0.5))} - k_{RORGT}*[RORGT],\\
\frac{d[IL21]}{dt} &= \frac{1}{1+exp(-b*(w_{IL21}-0.5))} - k_{IL21}*[IL21],\\
\frac{d[FOXP3]}{dt} &= \frac{1}{1+exp(-b*(w_{FOXP3}-0.5))} - k_{FOXP3}*[FOXP3],\\
\frac{d[TGFB]}{dt} &= \frac{1}{1+exp(-b*(w_{TGFB}-0.5))} - k_{TGFB}*[TGFB],\\
\frac{d[IL10]}{dt} &= \frac{1}{1+exp(-b*(w_{IL10}-0.5))} - k_{IL10}*[IL10],\\
\frac{d[IL9]}{dt} &= \frac{1}{1+exp(-b*(w_{IL9}-0.5))} - k_{IL9}*[IL9],\\
\frac{d[BCL6]}{dt} &= \frac{1}{1+exp(-b*(w_{BCL6}-0.5))} - k_{BCL6}*[BCL6].
\end{aligned}$$

$$\begin{aligned}
w_{TBET} = (&([IFNG] + p_{IL12e}*(1-[IL21])*(1-[IL4])*(1-[IL10])\\
&-[IFNG]*p_{IL12e}*(1-[IL21])*(1-[IL4])*(1-[IL10])
\end{aligned}$$

$$
\begin{aligned}
&+[TBET]-([IFNG]+p_{IL12e}*(1-[IL21])*(1-[IL4])*(1-[IL10])\\
&-[IFNG]*p_{IL12e}*(1-[IL21]))*(1-[IL4])*(1-[IL10])*[TBET])\\
&*(1-IL4)*(1-GATA3)*(1-IL21)*(1-BCL6)),\\
w_{IFNG} &= (p_{IFNGe}+([IFNG]+[TBET]-[IFNG]*[TBET])*(1-[GATA3])\\
&*(1-[TGFB])-p_{IFNGe}*([IFNG]+[TBET]-[IFNG]*[TBET])\\
&*(1-[GATA3])*(1-[TGFB])*(1-[IL21])*(1-[IL4])\\
&*(1-[IL10])*(1-[BCL6])*(1-[IL9])),\\
w_{GATA3} &= (([IL2]*[IL4]+[IL4]-[IL2]*[IL4]*[IL4])+[GATA3]\\
&-([IL2]*[IL4]+[IL4]-[IL2]*[IL4]*[IL4])*[GATA3])\\
&*(1-[TBET])*(1-[TGFB])*(1-[IL21])*(1-[IFNG])\\
&*(1-[BCL6]),\\
w_{IL2} &= ((p_{IL2e}+[IL2]*(1-[FOXP3])-p_{IL2e}*[IL2]*(1-[FOXP3]))(1-[INFG]))\\
&*(1-[IL21])*([FOXP3]+(1-[IL10])-[FOXP3]*(1-[IL10])),\\
w_{IL4} &= (p_{IL4e}+[GATA3]*([IL2]+[IL4]-[IL2]*[IL4])*(1-[TBET])\\
&-p_{IL4e}*[GATA3]*([IL2]+[IL4]-[IL2]*[IL4])*(1-[TBET]))\\
&*(1-[IFNG])*(1-[IL21]),\\
w_{TBET} &= (([IFNG]+p_{IL12e}*(1-[IL21])*(1-[IL4])*(1-[IL10])\\
&-[IFNG]*p_{IL12e}*(1-[IL21])*(1-[IL4])*(1-[IL10])\\
&+[TBET]-([IFNG]+p_{IL12e}*(1-[IL21])*(1-[IL4])*(1-[IL10])\\
&-[IFNG]*p_{IL12e}*(1-[IL21]))*(1-[IL4])*(1-[IL10])*[TBET])\\
&*(1-IL4)*(1-GATA3)*(1-IL21)*(1-BCL6)),\\
w_{IFNG} &= (p_{IFNGe}+([IFNG]+[TBET]-[IFNG]*[TBET])*(1-[GATA3])\\
&*(1-[TGFB])-p_{IFNGe}*([IFNG]+[TBET]-[IFNG]*[TBET])\\
&*(1-[GATA3])*(1-[TGFB])*(1-[IL21])*(1-[IL4])\\
&*(1-[IL10])*(1-[BCL6])*(1-[IL9])),\\
w_{GATA3} &= (([IL2]*[IL4]+[IL4]-[IL2]*[IL4]*[IL4])+[GATA3]\\
&-([IL2]*[IL4]+[IL4]-[IL2]*[IL4]*[IL4])*[GATA3])\\
&*(1-[TBET])*(1-[TGFB])*(1-[IL21])*(1-[IFNG])\\
&*(1-[BCL6]),\\
w_{IL2} &= ((p_{IL2e}+[IL2]*(1-[FOXP3])-p_{IL2e}*[IL2]*(1-[FOXP3]))(1-[INFG]))\\
&*(1-[IL21])*([FOXP3]+(1-[IL10])-[FOXP3]*(1-[IL10])),\\
w_{IL4} &= (p_{IL4e}+[GATA3]*([IL2]+[IL4]-[IL2]*[IL4])*(1-[TBET])\\
&-p_{IL4e}*[GATA3]*([IL2]+[IL4]-[IL2]*[IL4])*(1-[TBET]))
\end{aligned}
$$

$$
\begin{aligned}
&* (1 - [IFNG]) * (1 - [IL21]),\\
w_{RORGT} &= [IL21] * [TGFB] * (1 - [TBET]) * (1 - [FOXP3]) * (1 - [GATA3])\\
&* (1 - [BCL6]),\\
w_{IL21} &= ((((p_{IL6e} + p_{IL21e} - p_{IL6e} * p_{IL21e}) + [IL21] - (p_{IL6e} + p_{IL21e} - p_{IL6e} * p_{IL21e}) * [IL21])\\
&+ [RORGT] - ((p_{IL6e} + p_{IL21e} - p_{IL6e} * p_{IL21e}) + [IL21] - (p_{IL6e} + p_{IL21e} - p_{IL6e} * p_{IL21e})\\
&* [IL21]) * [RORGT]) + [BCL6] - (((p_{IL6e} + p_{IL21e} - p_{IL6e} * p_{IL21e}) + [IL21]\\
&- (p_{IL6e} + p_{IL21e} - p_{IL6e} * p_{IL21e}) * [IL21]) + [RORGT] - ((p_{IL6e} + p_{IL21e} - p_{IL6e} * p_{IL21e})\\
&+ [IL21] - (p_{IL6e} + p_{IL21e} - p_{IL6e} * p_{IL21e}) * [IL21]) * [RORGT]) * [BCL6])\\
&* (1 - [IFNG]) * (1 - [IL4]) * (1 - [IL10]) * (1 - [IL2]) * (1 - [IL9]),\\
w_{FOXP3} &= [IL2] * ([TGFB] + [FOXP3] - [TGFB] * [FOXP3]) * (1 - [IL21])\\
&* (1 - [RORGT]) * (1 - [IL4]),\\
w_{IL9} &= [IL4] * ([IL10] * [IL2] + [TGFB] - [IL10] * [IL2] * [TGFB])\\
&* (1 - [IFNG]) * (1 - [IL21]) * (1 - [FOXP3]),\\
w_{BCL6} &= ([IL21] + [IFNG] - [IL21] * [IFNG]) * (1 - [TBET]) * (1 - [IL2])\\
&* (1 - [TGFB]),\\
w_{TGFB} &= p_{TGFBe} + ([TGFB] + [FOXP3] - [TGFB] * [FOXP3]) * (1 - [IL21])\\
&- p_{TGFBe} * ([TGFB] + [FOXP3] - [TGFB] * [FOXP3]) * (1 - [IL21]),\\
w_{IL10} &= p_{IL10e} + [IL10]\\
&* (((([IFNG] + [IL21] - [IFNG] * [IL21]) + [TGFB] - ([IFNG] + [IL21]\\
&- [IFNG] * [IL21]) * [TGFB]) + [GATA3] - (([IFNG] + [IL21] - [IFNG] * [IL21])\\
&+ [TGFB] - ([IFNG] + [IL21] - [IFNG] * [IL21]) * [TGFB]) * [GATA3]) + p_{IL27e}\\
&- ((([IFNG] + [IL21] - [IFNG] * [IL21]) + [TGFB] - ([IFNG] + [IL21]\\
&- [IFNG] * [IL21]) * [TGFB]) + [GATA3] - (([IFNG] + [IL21] - [IFNG] * [IL21])\\
&+ [TGFB] - ([IFNG] + [IL21] - [IFNG] * [IL21]) * [TGFB]) * [GATA3]) * p_{IL27e}\\
&- p_{IL10e} * [IL10] * ((((([IFNG] + [IL21] - [IFNG] * [IL21]) + [TGFB] - ([IFNG]\\
&+ [IL21] - [IFNG] * [IL21]) * [TGFB]) + [GATA3] - (([IFNG] + [IL21]\\
&- [IFNG] * [IL21]) + [TGFB] - ([IFNG] + [IL21] - [IFNG] * [IL21]) * [TGFB])\\
&* [GATA3]) + p_{IL27e} - ((([IFNG] + [IL21] - [IFNG] * [IL21]) + [TGFB]\\
&- ([IFNG] + [IL21] - [IFNG] * [IL21]) * [TGFB]) + [GATA3] - (([IFNG]\\
&+ [IL21] - [IFNG] * [IL21]) + [TGFB] - ([IFNG] + [IL21] - [IFNG] * [IL21])\\
&* [TGFB]) * [GATA3]) * p_{IL27e}).
\end{aligned}
$$

**Acknowledgements**
Not applicable.

**Author contributions**
XL: Methodology, Formal analysis, Writing-Original Draft. QH: Formal analysis. ZX: Formal analysis. RW: Conceptualization, Writing-Review & Editing. All authors read and approved the final manuscript.

**Funding**
This work was supported by the National Natural Science Foundation of China [Grants No. 12371497].

**Data availability**
All data used and analyzed during the current study are available in MATLAB. The code is compiled using MATLAB. Furthermore, the materials mentioned in this study are included in the Appendix.

## Declarations

**Competing interests**
The authors declare no competing interests.

Received: 16 October 2024 Accepted: 12 January 2025 Published online: 03 February 2025

**References**

1. Bargaje, R., Trachana, K., Shelton, M.N., McGinnis, C.S., Zhou, J.X., Chadick, C., Cook, S., Cavanaugh, C., Huang, S., Hood, L.: Cell population structure prior to bifurcation predicts efficiency of directed differentiation in human induced pluripotent cells. Proc. Natl. Acad. Sci. **114**, 2271–2276 (2017)
2. Beriou, G., Bradshaw, E.M., Lozano, E., Costantino, C.M., Hastings, W.D., Orban, T., Elyaman, W., Khoury, S.J., Kuchroo, V.K., Baecher-Allan, C., et al.: TGF-$\beta$ induces IL-9 production from human Th17 cells. J. Immunol. **185**, 46–54 (2010)
3. Bettelli, E., Carrier, Y., Gao, W., Korn, T., Strom, T., Oukka, M., Kuchroo, V.: Reciprocal developmental pathways for the generation of pathogenic effector TH17 and regulatory T cells. Nature **441**, 235–238 (2006)
4. Borst, J., Ahrends, T., Bąbała, N., Melief, C.J., Kastenmüller, W.: CD4+ T cell help in cancer immunology and immunotherapy. Nat. Rev. Immunol. **18**, 635–647 (2018)
5. Bose, I., Pal, M.: Criticality in cell differentiation. J. Biosci. **42**, 683–693 (2017)
6. Burke, M.A., Morel, B.F., Oriss, T.B., Bray, J., McCarthy, S.A., Morel, P.A.: Modeling the proliferative response of T cells to IL-2 and IL-4. Cell. Immunol. **178**, 42–52 (1997)
7. Choi, J., Lysakovskaia, K., Stik, G., Demel, C., Söding, J., Tian, T.V., Graf, T., Cramer, P.: Evidence for additive and synergistic action of mammalian enhancers during cell fate determination. eLife **10**, e65381 (2021)
8. Chou, T.: Theoretical basis, experimental design, and computerized simulation of synergism and antagonism in drug combination studies. Pharmacol. Rev. **58**, 621–681 (2006)
9. Chou, T., Talalay, P.: Analysis of combined drug effects: a new look at a very old problem. Trends Pharmacol. Sci. **4**, 450–454 (1983)
10. Christie, D., Zhu, J.: Transcriptional regulatory networks for CD4 T cell differentiation. Curr. Top. Microbiol. Immunol. **381**, 125–172 (2014)
11. Eto, D., Lao, C., DiToro, D., Barnett, B., Escobar, T.C., Kageyama, R., Yusuf, I., Crotty, S.: IL-21 and IL-6 are critical for different aspects of B cell immunity and redundantly induce optimal follicular helper CD4 T cell (Tfh) differentiation. PLoS ONE **6**, e17739 (2011)
12. Fathman, C.G., Lineberry, N.B.: Molecular mechanisms of CD4+ T-cell anergy. Nat. Rev. Immunol. **7**, 599–609 (2007)
13. Ferrell, J.E., Ha, S.H.: Ultrasensitivity part I: Michaelian responses and zero-order ultrasensitivity. Trends Biochem. Sci. **39**, 496–503 (2014)
14. Fischer, H.P.: Mathematical modeling of complex biological systems: from parts lists to understanding systems behavior. Alcohol Res. Health **31**, 49 (2008)
15. Fisette, O., Patrick Lagüe, S.G., Morin, S.: Synergistic applications of MD and NMR for the study of biological systems. BioMed Res. Int. (2012)
16. Freudenberg, K., Lindner, N., Dohnke, S., Garbe, A.I., Schallenberg, S., Kretschmer, K.: Critical role of TGF-$\beta$ and IL-2 receptor signaling in Foxp3 induction by an inhibitor of DNA methylation. Front. Immunol. **9**, 125 (2018)
17. Geginat, J., Paroni, M., Maglie, S., Alfen, J.S., Kastirr, I., Gruarin, P., De Simone, M., Pagani, M., Abrignani, S.: Plasticity of human CD4 T cell subsets. Front. Immunol. **5**, 630 (2014)
18. Gol-Ara, M., Jadidi-Niaragh, F., Sadria, R., Azizi, G., Mirshafiey, A.: The role of different subsets of regulatory T cells in immunopathogenesis of rheumatoid arthritis. Arthritis **2012**, 805875 (2012)
19. Gorochov, G., Neumann, A.U., Kereveur, A., Parizot, C., Li, T., Katlama, C., Karmochkine, M., Raguin, G., Autran, B.: Perturbation of CD4+ and CD8+ T-cell repertoires during progression to AIDS and regulation of the CD4+ repertoire during antiviral therapy. Nat. Med. **4**, 215–221 (1998)
20. Grazia Roncarolo, M., Gregori, S., Battaglia, M., Bacchetta, R., Fleischhauer, K., Levings, M.K.: Interleukin-10-secreting type 1 regulatory T cells in rodents and humans. Immunol. Rev. **212**, 28–50 (2006)
21. Haghverdi, L., Büttner, M., Wolf, F.A., Buettner, F., Theis, F.J.: Diffusion pseudotime robustly reconstructs lineage branching. Nat. Methods **13**, 845–848 (2016)
22. Haney, S., Bardwell, L., Nie, Q.: Ultrasensitive responses and specificity in cell signaling. BMC Syst. Biol. **4**, 1–14 (2010)
23. Hirsch, M.W.: The dynamical systems approach to differential equations. Bull. Am. Math. Soc. **11**, 1–64 (1984)
24. Hu, Q., Tang, R., He, X., Wang, R.: General relationship of local topologies, global dynamics, and bifurcation in cellular networks. npj Syst. Biol. Appl. **10**, 135 (2024)
25. Johnston, R.J., Poholek, A.C., DiToro, D., Yusuf, I., Eto, D., Barnett, B., Dent, A.L., Craft, J., Crotty, S.: Bcl6 and Blimp-1 are reciprocal and antagonistic regulators of T follicular helper cell differentiation. Science **325**, 1006–1010 (2009)
26. Kakaradov, B., Arsenio, J., Widjaja, C.E., He, Z., Aigner, S., Metz, P.J., Yu, B., Wehrens, E.J., Lopez, J., Kim, S.H., et al.: Early transcriptional and epigenetic regulation of CD8+ T cell differentiation revealed by single-cell RNA sequencing. Nat. Immunol. **18**, 422–432 (2017)

27. Kanhere, A., Hertweck, A., Bhatia, U., Gökmen, M.R., Perucha, E., Jackson, I., Lord, G.M., Jenner, R.G.: T-bet and GATA3 orchestrate Th1 and Th2 differentiation through lineage-specific targeting of distal regulatory elements. Nat. Commun. **3**, 1268 (2012)
28. Lähnemann, D., Köster, J., Szczurek, E., McCarthy, D.J., Hicks, S.C., Robinson, M.D., Vallejos, C.A., Campbell, K.R., Beerenwinkel, N., Mahfouz, A., et al.: Eleven grand challenges in single-cell data science. Genome Biol. **21**, 1–35 (2020)
29. Lexberg, M.H., Taubner, A., Albrecht, I., Lepenies, I., Richter, A., Kamradt, T., Radbruch, A., Chang, H.D.: IFN-$\gamma$ and IL-12 synergize to convert in vivo generated Th17 into Th1/Th17 cells. Eur. J. Immunol. **40**, 3017–3027 (2010)
30. Luo, M., Huang, D., Jiao, J., Wang, R.: Detection of synergistic combinatorial perturbations by a bifurcation-based approach. Int. J. Bifurc. Chaos **31**, 2150175 (2021)
31. Luongo, A., Paolone, A.: Perturbation methods for bifurcation analysis from multiple nonresonant complex eigenvalues. Nonlinear Dyn. **14**, 193–210 (1997)
32. Marco, E., Karp, R.L., Guo, G., Robson, P., Hart, A.H., Trippa, L., Yuan, G.C.: Bifurcation analysis of single-cell gene expression data reveals epigenetic landscape. Proc. Natl. Acad. Sci. **111**, E5643–E5650 (2014)
33. Martinez-Sanchez, M.E., Huerta, L., Alvarez-Buylla, E.R., Villarreal Luján, C.: Role of cytokine combinations on CD4+ T cell differentiation, partial polarization, and plasticity: continuous network modeling approach. Front. Physiol. **9**, 339229 (2018)
34. Martinez-Sanchez, M.E., Mendoza, L., Villarreal, C., Alvarez-Buylla, E.R.: A minimal regulatory network of extrinsic and intrinsic factors recovers observed patterns of CD4+ T cell differentiation and plasticity. PLoS Comput. Biol. **11**, e1004324 (2015)
35. Mosmann, T.R., Coffman, R.L.: TH1 and TH2 cells: different patterns of lymphokine secretion lead to different functional properties. Annu. Rev. Immunol. **7**, 145–173 (1989). https://doi.org/10.1146/annurev.iy.07.040189.001045
36. Murphy, K., Weaver, C.: Janeway's Immunobiology. Garland Science (2016)
37. Murugaiyan, G., Mittal, A., Lopez-Diego, R., Maier, L.M., Anderson, D.E., Weiner, H.L.: IL-27 is a key regulator of IL-10 and IL-17 production by human CD4+ T cells. J. Immunol. **183**, 2435–2443 (2009)
38. Nakajima, A., Kaneko, K.: Regulative differentiation as bifurcation of interacting cell population. J. Theor. Biol. **253**, 779–787 (2008)
39. O'Shea, J.J., Paul, W.E.: Mechanisms underlying lineage commitment and plasticity of helper CD4+ T cells. Science **327**, 1098–1102 (2010)
40. Perez, V.L., Lederer, J.A., Lichtman, A.H., Abbas, A.K.: Stability of Th1 and Th2 populations. Int. Immunol. **7**, 869–875 (1995)
41. Perko, L.: Differential Equations and Dynamical Systems, vol. 7. Springer, Berlin (2013)
42. Sakaguchi, S., Yamaguchi, T., Nomura, T., Ono, M.: Regulatory T cells and immune tolerance. Cell **133**, 775–787 (2008)
43. Sallusto, F., Monticelli, S.: The many faces of CD4 T cells: roles in immunity and disease. In: Seminars in Immunology, pp. 249–251 (2013)
44. Sastry, S.: Nonlinear Systems: Analysis, Stability, and Control, vol. 10. Springer, Berlin (2013)
45. Tang, R., He, X., Wang, R.: Constructing maps between distinct cell fates and parametric conditions by systematic perturbations. Bioinformatics **39**, btad624 (2023)
46. Vahedi, G., Kanno, Y., Sartorelli, V., O'Shea, J.J.: Transcription factors and CD4 T cells seeking identity: masters, minions, setters and spikers. Immunology **139**, 294–298 (2013)
47. Villarreal, C., Padilla-Longoria, P., Alvarez-Buylla, E.: General theory of genotype to phenotype mapping: derivation of epigenetic landscapes from N-node complex gene regulatory networks. Phys. Rev. Lett. **109**, 118102 (2012)
48. Wang, W., Ma, W., Feng, Z.: Complex dynamics of a time periodic nonlocal and time-delayed model of reaction–diffusion equations for modeling CD4+ T cells decline. J. Comput. Appl. Math. **367**, 112430 (2020)
49. Yamane, H., Paul, W.E.: Early signaling events that underlie fate decisions of naive CD4+ T cells toward distinct T-helper cell subsets. Immunol. Rev. **252**, 12–23 (2013)
50. Yan, F., Liu, H., Liu, Z.: Dynamic analysis of the combinatorial regulation involving transcription factors and microRNAs in cell fate decisions. Biochim. Biophys. Acta, Proteins Proteomics **1844**, 248–257 (2014)
51. Yusuf, A.A., Figueiredo, I.P., Afsar, A., Burroughs, N.J., et al.: The effect of a linear tuning between the antigenic stimulations of CD4+ T cells and CD4+ Tregs. Mathematics **8**, 293 (2020)
52. Zhang, Q., Bhattacharya, S., Andersen, M.E.: Ultrasensitive response motifs: basic amplifiers in molecular signalling networks. Open Biol. **3**, 130031 (2013)
53. Zhou, L., Chong, M.M., Littman, D.R.: Plasticity of CD4+ T cell lineage differentiation. Immunity **30**, 646–655 (2009)
54. Zhou, L., Shi, Y.L., Li, K., Hamzavi, I., Gao, T.W., Huggins, R.H., Lim, H.W., Mi, Q.S.: Increased circulating Th17 cells and elevated serum levels of TGF-beta and IL-21 are correlated with human non-segmental vitiligo development. Pigment Cell Melanoma Res. **28**, 324–329 (2015)
55. Zhu, J., Paul, W.E.: Peripheral CD4+ T-cell differentiation regulated by networks of cytokines and transcription factors. Immunol. Rev. **238**, 247–262 (2010)
56. Zhu, J., Yamane, H., Paul, W.E.: Differentiation of effector CD4 T cell populations. Annu. Rev. Immunol. **28**, 445–489 (2009)


## Publisher's Note